Novel *N*-Acyl Hydrazone Compounds as Promising Anticancer Agents: Synthesis and Molecular Docking Studies

Yağmur Biliz, Belma Hasdemir,* Hatice Başpınar Küçük, Merve Zaim, Ahmet Mesut Şentürk, Aynur Müdüroğlu Kırmızıbekmez, and İhsan Kara
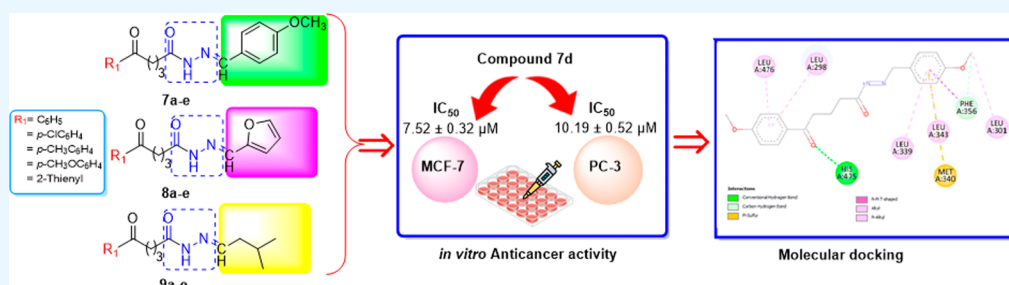
Read Online

ACCESS | Metrics & More | Article Recommendations | SI Supporting Information

ABSTRACT: In this study, a new series of *N*-acyl hydrazones **7a-e**, **8a-e**, and **9a-e**, starting from methyl δ-oxo pentanoate with different substituted groups **1a-e**, were synthesized as anticancer agents. The structures of obtained target molecules were identified by spectrometric analysis methods (FT-IR, ^{11}H NMR, ^{13}C NMR, and LC−MS). The antiproliferative activity of the novel *N*-acyl hydrazones was evaluated on the breast (MCF-7) and prostate (PC-3) cancer cell lines by an MTT assay. Additionally, breast epithelial cells (ME-16C) were used as reference normal cells. All newly synthesized compounds **7a-e**, **8a-e**, and **9a-e** exhibited selective antiproliferative activity with high toxicity to both cancer cells simultaneously without any toxicity to normal cells. Among these novel *N*-acyl hydrazones, **7a-e** showed the most potent anticancer activities with IC$_{50}$ values at 7.52 ± 0.32−25.41 ± 0.82 and 10.19 ± 0.52−57.33 ± 0.92 μM against MCF-7 and PC-3 cells, respectively. Also, molecular docking studies were applied to comprehend potential molecular interactions between compounds and target proteins. It was seen that the docking calculations and the experimental data are in good agreement.

1. INTRODUCTION

Today, one of the main causes of death worldwide is cancer, which develops when one or more cells from a certain tissue in the body deviate from their usual properties and multiply uncontrollably.[1,2] According to the findings of recent studies, female breast cancer is the most commonly diagnosed cancer, with 11.7% of cases and 6.9% of all cancer deaths, followed by lung (11.4%), colorectal (10.0%), prostate (7.3%), and stomach (5.6%) cancers.[3,4]

In recent years, intensive studies have been carried out around the world for the development of new drugs that can act against cancer. Today, many factors, such as the rapidly increasing number of patients, serious side effects caused by drugs in use, toxicity, and the development of drug resistance by tumors, increase the importance of these studies. Chemotherapy, one of the anticancer treatments, is widely used because of its effects on tumor cells. However, it is known that many anticancer drugs have serious adverse effects and toxicity. Therefore, it is of great importance to develop new anticancer agents that can stop the growth of cancer cells or kill them while at the same time not harming healthy cells.

Small organic compounds serve as bioactive scaffolds, which are a crucial component of drug design. *N*-Acyl hydrazones, which are an important member of the class of organic compounds and are represented by the general formula R$_1$−NHN═CH−R$_2$, are small organic molecules in which R$_1$ and R$_2$ represent different functional groups. In recent years, the interest of researchers has focused on *N*-acyl hydrazones, which have very important pharmacological properties, thus a good option for the development of new biologically active drug molecules.[5−13]

In the research carried out to find more effective and, at the same time, low-toxic anticancer drugs, it was determined that *N*-acyl hydrazone derivatives have anticancer activity, and this result increased the importance of this substance group in cancer treatment. In the literature survey, it is observed that
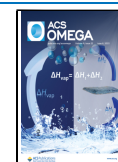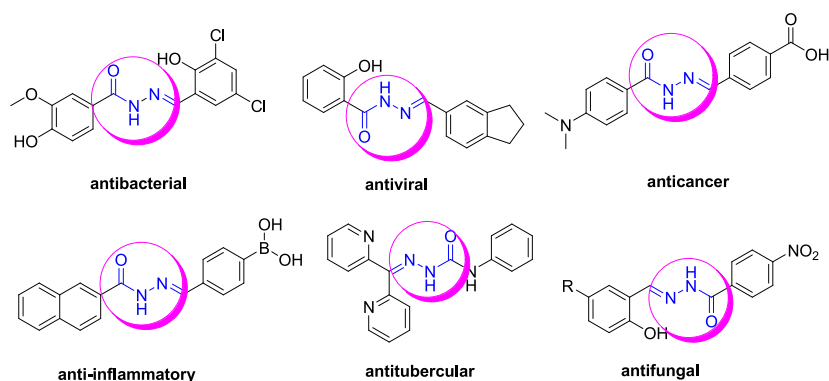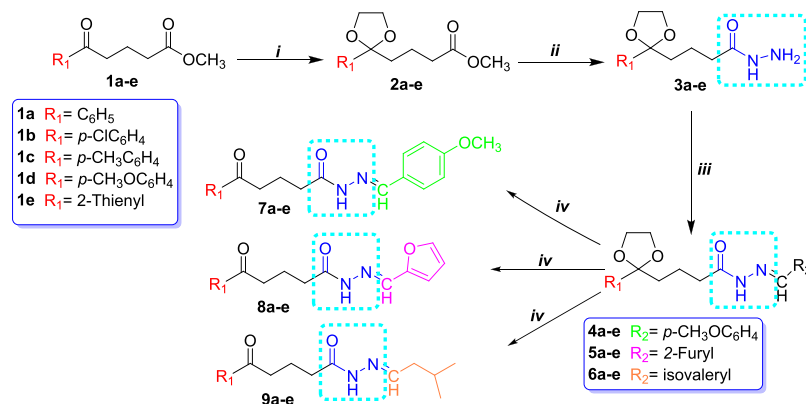
Figure 1. Some *N*-acyl hydrazone compounds for specific targeting applications.

Scheme 1. Synthetic Route Was Followed for the Synthesis of the Novel *N*-Acyl Hydrazones[a]

[a]Reagents and conditions: (i) Ethylene glycol, triethyl orthoformate, *p*-toluenesulfonic acid monohydrate, toluene, reflux, 24 h (90−96%); (ii) hydrazine monohydrate, EtOH, reflux, 6 h (95−98%); (iii) R₂CHO (R₂ = *p*-MeOC₆H₄ **4a-e**; 2-furyl **5a-e**; isovaleryl **6a-e**), DMF, reflux (51−95%); (iv) Bi(NO₃)₃·5H₂O, CH₂Cl₂, rt., 2−4 h (98%).

new derivatives of *N*-acyl hydrazones are prepared and their anticancer activities are measured, and these drugs are modified by preparing their analogues with commercially available anticancer drugs.[14−23] For example, in a study by Popiołek et al., *N*-acyl hydrazones derived from 3-hydroxy-2-naphthoic acid were found to show significant antitumor activities against HepG2 and 769-P cell lines.[24] In another study, a series of *N*-acyl hydrazone derivatives synthesized from ethyl paraben were reported to have potential activity against liver cancer (HepG2).[25] The synthesized dipyrromethane *N*-acyl hydrazone derivatives exhibited moderate to extremely strong cytotoxic effects against HL-60 (leukemia) and HCT-116 (colon) cancer cells according to a different study by Gautam et al.[26] Novel (*R,S*)-etodolac derivatives containing the *N*-acyl hydrazone moiety synthesized by Koç et al. have been found to have good cytotoxic effects against PC-3, DU-145, and LNCaP cell lines (prostate cancer).[27]

Further, *N*-acyl hydrazones are well-known to exhibit a wide spectrum of biological properties as antioxidant,[28−31] analgesic,[32] anti-inflammatory,[33−35] antimicrobial,[36−41] antiviral,[42,43] anticonvulsant,[44] antiprotozoal,[45] antimalarial,[46] larvicidal,[47] antituberculosis,[48] and antifungal[49] activity. Some compounds with known biological activities containing the *N*-acyl hydrazone structure are shown in Figure 1.

In the previous study of our group, we synthesized γ- and δ-imino esters from γ- and δ-oxo methyl ester derivatives and found that they exhibited high antioxidant activity.[50] In another study, we obtained γ-oxime esters and determined

that they showed elastase inhibition activity.[51] Based on our previous studies and literature data, in this work, we focused to designing and synthesizing novel *N*-acyl hydrazones from methyl δ-oxo pentanoate with different substituted groups with promising considerable anticancer properties. For this purpose, we synthesized fifteen novel *N*-acyl hydrazone derivatives **7a-e**, **8a-e**, and **9a-e** from their corresponding methyl δ-oxo pentanoates with aryl, substituted aryl, and heteroaryl groups (Scheme 1). The structures of the compounds **7a-e**, **8a-e**, and **9a-e** were elucidated by FT-IR, ¹H NMR, ¹³C NMR, and LC−MS analysis methods, and their purity was confirmed by HPLC. Compounds **7a-e**, **8a-e**, and **9a-e** were screened for their in vitro anticancer activity against breast (MCF-7) and prostate (PC-3) cancer cell lines using a 3-(4,5-dimethylthiazol-2-yl)-2,5- diphenyltetrazolium bromide (MTT) assay. In addition, molecular docking studies were applied to investigate the antiproliferative effects of these novel compounds.

2. RESULTS AND DISCUSSION

2.1. Chemistry. In this study, we synthesized fifteen new *N*-acyl hydrazones **7a-e**, **8a-e**, and **9a-e** derived from methyl δ-oxo pentanoates with aryl, substituted aryl, and heteroaryl groups **1a-e** (Scheme 1).

First, we obtained the methyl δ-oxo pentanoate derivatives with substituted aryl and heteroaryl groups **1b-e** used as starting compounds according to the Friedel−Crafts acylation reaction in 85−90% yield.[52,53] Compound **1a** was obtained from the reaction of δ-oxo-δ-phenyl-pentanoic acid with

methanol in the presence of concentrated sulfuric acid in 100% yield. Next, compounds **1a-e** were reacted with hydrazine monohydrate in ethanol in order to obtain δ-oxo pentane hydrazide derivatives as the key intermediate. When we examined the reaction of similar molecules with hydrazine in the literature, we saw that the reaction was carried out without protecting the carbonyl group.[54,55] However, in our experiments, we observed that both C=O groups in the molecule reacted with hydrazine hydrate, thus reducing the reaction efficiency (45−50%). Thus, we decided to protect the carbonyl group in the δ-position in order to increase the reaction yield and prevent the formation of byproducts. A model reaction was used to determine optimum reaction conditions; we reacted compound **1a** with varying molar ratios of ethylene glycol (EG), triethyl orthoformate (TMOF), and p-toluene-sulfonic acid monohydrate (p-TsOH). The results are given in Table 1. In Table 1, entry 2 shows that the reaction was
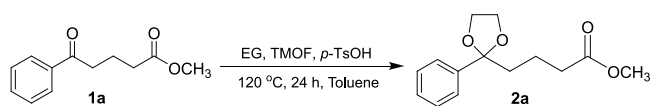
Table 1. Reaction Condition Experiments for Ketalization

entry	1a:EG	1a:TMOF	1a:p-TsOH	conv. (%)[a]
			molar ratio	
1	1:1.1	1:0	1:0.05	25
2	**1:3**	**1:3**	**1:0.01**	**96**
3	1:5	1:3	1:0.01	75
4	1:5	1:3	1:0.1	82

[a]Determined by GC−MS

performed with molar ratios of 1:3:3:0.01 **1a**/EG/TMOF/p-TsOH with a 96% yield. Therefore, compounds **2a-e** were successfully obtained in 90−96% isolated yields. Product formation was determined by the GC−MS chromatographic method. Then, ketal the intermediates **3a-e** were prepared by refluxing compounds **2a-e** with hydrazine monohydrate in ethanol in 95−98% yields. The formation of the intermediates **3a-e** was confirmed by the molecular ion peak observed by the GC−MS spectrum. Finally, compounds **3a-e** were reacted with various aldehydes (p-anisaldehyde, 2-furaldehyde, and iso-valeraldehyde) in dimethylformamide (DMF) in the refluxing condition to generate δ-ketal N-acyl hydrazones **4a-e**, **5a-e**, and **6a-e** in 51−95% isolated yields.[56,57] Then, the hydrolysis reaction of **4a** was investigated in the presence of several acid catalysts and solvents in order to optimize reaction conditions. The results are shown in Table 2. In Table 2, entry 4 shows that the reaction was carried out in the presence of Bi(NO₃)₃·

5H₂O in CH₂Cl₂ at room temperature with a 98% yield. According to these reaction conditions, N-acyl hydrazone derivatives **7a-e**, **8a-e**, and **9a-e** were obtained with 95−98% isolated yields. All the target molecules **7a-e**, **8a-e**, and **9a-e** are shown in Figure 2.

The molecular structures of synthesized N-acyl hydrazones **7a-e**, **8a-e**, and **9a-e** were identified through spectroscopic methods (Figures S1−S45, Supporting Information). The purity of these compounds was determined at 97.8−100% by HPLC analysis (Figures S46−S60, Supporting Information).

In the FT-IR spectra, weak −NH bands were observed at 3279−3172 cm^{-1} and N−N bands at 1178−1015 cm^{-1} in all target compounds. Carbonyl absorption (C=O), belonging to both the azomethine group and the aliphatic chain, was seen between 1515−1477 and 1684−1556 cm^{-1}, respectively. The peaks around 1596−1488 cm^{-1} are evidence of the presence of the C=N group. The peaks of aromatic ring vibrations were observed between 3090−3026 and 1608−1538 cm^{-1}. The literature suggests that the hydrazones could exist as cis/trans amide conformers and E/Z geometrical isomers centered on C−N double bonds.[25,58] In the present study, the peaks observed in the ^{1}H and ^{13}C NMR spectra of the N-acyl hydrazone compounds showed that **7a-e** and **8a-e** were obtained as a mixture of E and Z isomers. However, compounds **9a-e** were determined to be in single isomer form. Therefore, we evaluated the signals of the ^{1}H NMR spectra of the compounds **7a-e** and **8a-e** as set I and set II.[58] In each compound's ^{1}H NMR spectrum for **7a-e**, **8a-e**, and **9a-e**, the characteristic signals of the azomethine =CH protons found at δ 11.23−8.98 ppm were observed as broad singlets and those of −NH amide protons (−CONHNCH−) as singlets and triplets at δ 7.89−7.09 ppm. Aromatic protons are seen as a doublet, triplet, and multiplet between δ 7.98 and 6.56 ppm. The chemical shift and integral values of other protons are in agreement with their compound structures. In the ^{13}C NMR spectra, the azomethine group (−N=CH−) signals were detected at δ 168.7−146.3 ppm. The signals corresponding to C=O of ester and amide were observed at δ 200.2−192.7 and δ 175.2−174.2 ppm, respectively. Other aliphatic and aromatic carbon signals of N-acyl hydrazones **7a-e**, **8a-e**, and **9a-e** were seen at the expected values of chemical shift.

2.2. Cytotoxicity Assay. In this work, cells were treated with the compounds at concentrations ranging from 1 to 1000 M for 48 h in order to evaluate the in vitro cytotoxic effects on cancer (MCF-7, PC-3) and normal (ME-16C) cell lines. Doxorubicin, the most commonly used chemotherapy drug to treat various types of cancer cells, was chosen as the positive
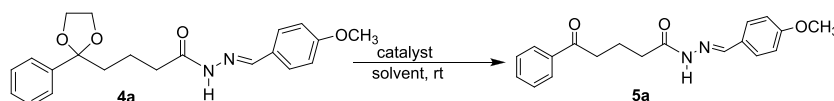
Table 2. Reaction Condition Experiments for Deprotection of Ketal N-Acyl Hydrazones

entry	catalyst	solvent	time	conv (%)[e]	by product (conv. %)[e]
1	p-TsOH[a]	acetone:water	40 min	45	38
2	p-TsOH[b]	acetone:water	40 min	49	35
3	1 M HCl[c]	THF	3 h	—	—
4	**Bi(NO₃)₃·5H₂O[d]**	**CH₂Cl₂**	**2 h**	**98**	—

[a]Molar ratio of 4a:catalyst = 1:1. [b]Molar ratio of 4a:catalyst = 1:0.5. [c]Molar ratio of 4a:catalyst = 1:0.01. [d]Molar ratio of 4a:catalyst = 1:0.25. [e]Determined by GC−MS.
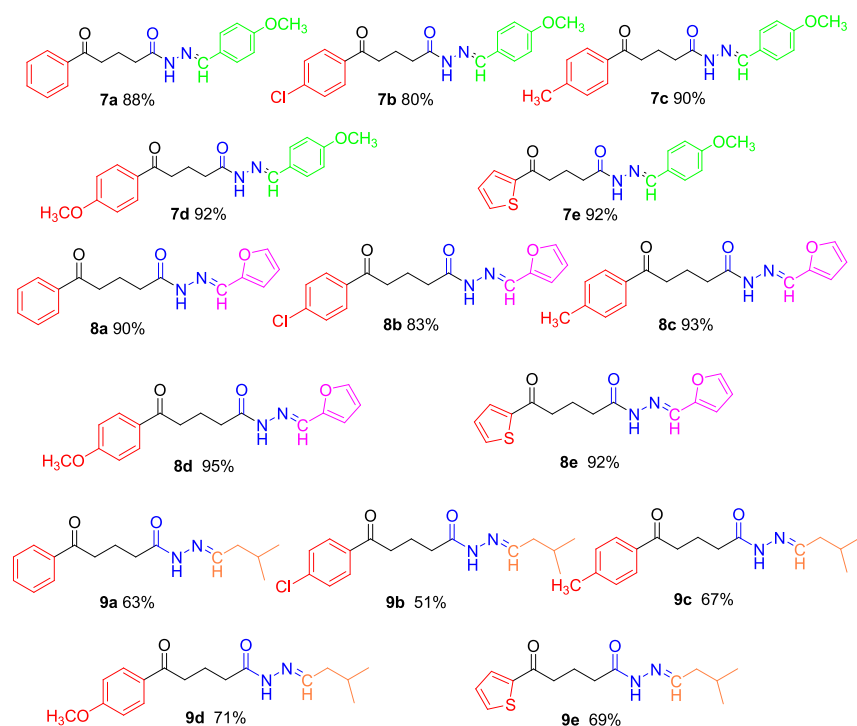
Figure 2. Structure of the target products.

Table 3. In Vitro Cytotoxic Activity of Newly Synthesized *N*-Acyl Hydrazone Derivatives[a]

		IC$_{50}$ (μM)		
entry	comp. no	MCF-7	PC-3	ME-16C
1	**7a**	**25.41 ± 0.82**	**57.33 ± 0.92**	**545.32 ± 0.75**
2	**7b**	**10.27 ± 0.63**	**15.00 ± 0.40**	**158.37 ± 1.90**
3	**7c**	**9.25 ± 0.54**	**12.57 ± 0.67**	**227.65 ± 1.76**
4	**7d**	**7.52 ± 0.32**	**10.19 ± 0.52**	**250.43 ± 1.88**
5	**7e**	**12.54 ± 0.84**	**10.81 ± 0.71**	**672.18 ± 2.69**
6	8a	10.98 ± 1.21	26.57 ± 0.92	471.76 ± 2.98
7	8b	50.75 ± 0.63	51.95 ± 0.88	ND
8	8c	471.53 ± 0.57	510.13 ± 1.10	480.53 ± 2.05
9	8d	510.19 ± 2.88	454.71 ± 2.31	ND
10	8e	490.65 ± 3.49	500.52 ± 2.83	ND
11	9a	120.25 ± 1.87	ND	ND
12	9b	210.00 ± 3.14	275.82 ± 5.9	ND
13	9c	95.02 ± 0.76	106.32 ± 3.7	ND
14	9d	115.95 ± 2.7	152.14 ± 0.75	ND
15	9e	100.08 ± 1.39	125.46 ± 1.1	ND
16	doxorubicin	0.83 ± 0.07	0.75 ± 0.04	0.80 ± 0.09

[a]IC$_{50}$: The concentration that inhibits 50% of cell proliferation; ND: Not determined; ± values represent the standard deviation of the mean.

control agent. According to the results, nearly all compounds possess cytotoxic activity against cancer cells with IC$_{50}$ values ranging from 7.52 ± 0.32 to 510.19 ± 2.88 μM (Table 3). Among selected cancer cell lines, MCF-7 cells were more sensitive to the antiproliferative effects of newly synthesized *N*-acyl hydrazones. Doxorubicin demonstrated significantly low IC$_{50}$ values at 0.83 ± 0.07, 0.75 ± 0.04, and 0.80 ± 0.09 for MCF-7, PC-3, and ME-16C cell lines, respectively (Table 3, entry 16). Although doxorubicin seems to be very effective in killing cancer cells at low concentrations, it is also highly toxic to normal cells at the same concentration.

Compounds **7a-e** exhibited more potent cytotoxic activity in cancer cells than compounds **8a-e** and **9a-e**. Therefore, the selectivity index (SI) of compounds **7a-e** was calculated and is presented in Figure 3. SI is a ratio of the IC$_{50}$ value in cancer cell lines (MCF-7, PC3) to the IC$_{50}$ value in non-cancer cell lines (ME16C). SI values greater than 1.0 demonstrate higher anticancer activity.[59] The data revealed that compound **7d** was the most cytotoxic compound with IC$_{50}$ values at 7.52 ± 0.32 and 10.19 ± 0.52 μM against MCF-7 and PC-3 cells, respectively (Table 3, entry 4). Moreover, **7d** selectively inhibited the growth of cancer cell lines exhibiting a SI of 33.30 and 24.57 for MCF-7 and PC-3 cells, respectively (Figure 3). **7e** was also characterized by high cytotoxicity and the greatest selectivity with 53.60 and 62.18 SI values for MCF-7 and PC-3 cells, respectively (Figure 3). These results suggest that compounds **7d** and **7e** are promising because of their elevated
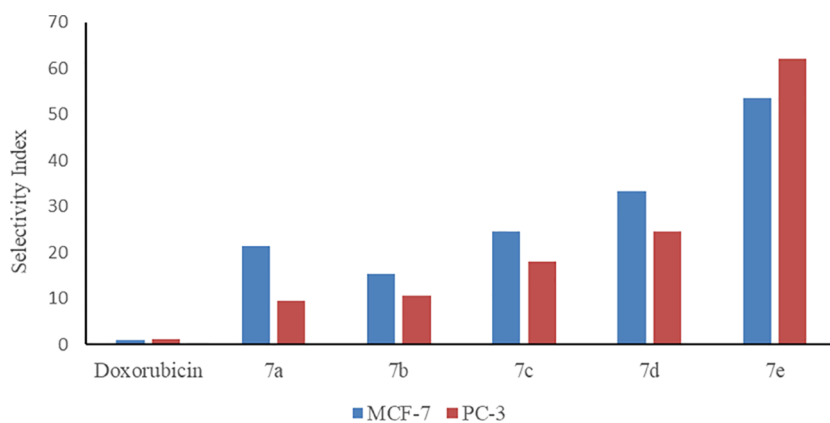
Figure 3. SI of synthesized *N*-acyl hydrazone derivatives **7a-e**.

antiproliferative activity along with considerable selectivity (Table 3, entry 5).

The cytotoxic activity of synthesized *N*-acyl hydrazones in cancer cell lines differed among cells. **7d**, **7c**, and **7b** exhibited the highest antiproliferative effects in MCF-7 cells, whereas **8c**, **8e**, and **8d** were the lowest toxic compounds, respectively. On the other hand, the cytotoxicity order differs in PC-3 cells as **7d**, **7e**, and **7c** were characterized as the most toxic compounds, whereas **8d**, **8e**, and **8c** were the least toxic compounds. The methoxy group in the phenyl ring attached to the azomethine group at the R_2 position activates the ring due to its electron donor effect. As a result of this effect, it can be assumed that compounds **7a-e** carrying the p-methoxy phenyl group in the R_2 position have higher antiproliferative activity than other compounds (**8a-e** and **9a-e**). Among synthesized *N*-acyl hydrazones, **8b**, **8d**, **8e**, and **9a-e** did not cause any cytotoxic effect in ME-16C cells in the tested range of concentrations. As a result, it was revealed that the *p*-methoxy phenyl group at the R_2 position ($R_1-NHN=CH-R_2$) is crucial for inducing cytotoxicity as well as selectivity against the MCF-7 cancer cell line. By replacing the *p*-methoxy phenyl group with furyl or isovaleryl groups, cytotoxic activities were reduced.

2.3. Molecular Docking Studies. By molecular docking experiments, these novel compounds' antiproliferative effects have been examined, and comprehensive evaluations of the molecules' ideal poses have been conducted. By evaluating the best binding affinity and receptor-ligand interaction of each compound, the good interactions of the compounds within the receptor active pocket of the target receptor proteins are shown in Tables 4 and 5. Considering prior studies of identical structures that contain hydrazone subunits, we made the decision to look for potential binding motifs for MCF-7 and PC-3 in order to examine their anticancer properties for breast cancer (MCF-7) and prostate cancer (PC-3).[60,61] Thus, the proteins with the highest affinity for the target molecules were determined as 1Z5M for PC-3 and 1X7B for MCF-7. Doxorubicin, an often-used anticancer medicine, was selected to compare our results.

After the docking interactions, the conformation with relatively low docking energy scores is selected because the ligand's strongest binding potential inside the target is indicated by the conformation with the lowest negative binding energy values.

Nearly all of the compounds demonstrated adequate binding free energies for MCF-7 and PC-3 that ranged between −9.67

and −11.74 and −7.28 and −9.37 Kcal/mol, respectively. Figures 4−7 show that the compounds bind to the active position and overlap with the reference compounds. According to our preliminary findings, these substances have a respectable level of ligand-receptor binding interactions.

Compounds **7b-d** and **8b** have the smallest RMSD scores with the lowest binding energy scores in each target. As shown in the tables, some of them also exhibited powerful hydrogen bonding with related amino acid residues. The figures show that the active conformations of each compound bind the active site and overlap with each other. The results established that these compounds forecasted the best ligand-receptor binding interactions. Additionally, we evaluated the interactions involved between the target proteins (1Z5M and 1X7B) and compound **7d** which exhibited high affinity toward 1Z5M and 1X7B and has proven to possess good in vitro anticancer activity. Figures 8 and 9 show the interactions between ligands and proteins. Compound **7d** interacts with nine residues to be complexed with 1Z5M as seen in Figure 8. It implicated five alkyl interactions with VAL A: 96, ALA A: 109, VAL A: 143, LEU A: 159, and ALA A: 162; one Pi-sigma interaction with LEU A: 212; attractive charges with GLU A:166 and hydrogen bonds with GLY A:165 and LEU A:88 residues which interact with compound **7d** were identified to be relevant in the complexation process between **7d** and 1Z5M. In Figure 9, compound **7d** interacts with eight residues to be complexed with 1X7B. It implicated five alkyl interactions with LEU A: 298, LEU A: 301, LEU A: 339, LEU A: 343, and LEU A: 476; one carbon-hydrogen bond with PHE A: 356; one pi-sulfur bond with MET A:340; and a hydrogen bond with HIS A:475.

2.4. Drug-like Properties. The Swiss ADME Calculation program has been used to determine drug-likeness rankings in order to better understand the structure−activity correlations of compounds. Table 6 lists the molecular weight, logP, TPSA, blood−brain barrier (BBB) crossing, GI absorption characteristics, and kind of CYPP450 inhibition of drugs. Almost all substances have been shown to have quite low levels that will cross lipid barriers. Compounds have been identified to have lipophilicity values less than 4.
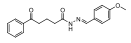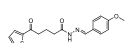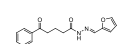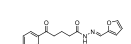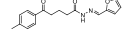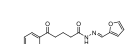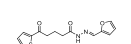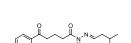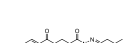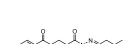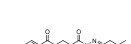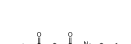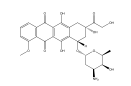
3. CONCLUSIONS

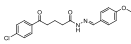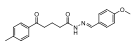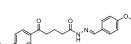In summary, we designed, synthesized, and identified novel *N*-acyl hydrazone derivatives **7a-e**, **8a-e**, and **9a-e** and tested them for in vitro cytotoxicity. Overall, this study presents evidence that *N*-acyl hydrazone derivatives exhibit significant and

Table 4. Results of MCF-7 Breast Cancer-1X7B Docking

Comp No.	Structures	Docked aminoacid residues (vdW interactions)	Energy Score	RMSD Value	H bond (distance Å)
7a		MET295, LEU298, ILE376, LEU476	−11.00	1.07	O of Carbonyl with H of NH of HIS475 (2.090)
7b		MET295, HIS475, LEU476	−11.31	1.04	None
7c		MET295, LEU298, ILE373, LEU476	−11.65	0.87	None
7d		LEU298, ARG346, LEU476	−11.74	0.65	O of Carbonyl with H of NH of HIS475 (2.080)
7e		ARG346, ILE373, HIS475	−10.57	1.24	None
8a		LEU298, THR289, ILE373, LEU476	−10.99	0.67	O of Carbonyl with H of NH of HIS475 (2.155)
8b		LEU298, THR289, ILE373, LEU476	−10.62	0.73	None
8c		ALA302, LEU343, ILE373	−11.59	0.77	None
8d		LEU298, ILE376, LEU380, LEU476	−10.89	1.34	O of Carbonyl with H of NH of HIS475 (1.855)
8e		MET295, LEU298, ILE373, LEU476	−9.84	1.10	O of Carbonyl with H of NH of HIS475 (1.914)
9a		MET295, LEU298, LEU476	−9.51	1.29	None
9b		MET295, LEU298, LEU476	−10.17	0.96	None
9c		LEU298, ILE373, HIS475, LEU476	−9.67	1.04	None
9d		MET295, LEU298, HIS475	−10.52	0.31	None
9e		MET295, LEU298, LEU476	−9.29	0.83	O of Carbonyl with H of NH of HIS475 (1.867)
Doxorubicin		MET295, LEU298, ILE373, LEU476	−12.89	0.89	H of OH with O of Carbonyl of LEU339 (1.816)

Table 5. Results of PC-3 Prostate Cancer-1Z5M Docking

Comp No.	Structures	Docked aminoacid residues (vdW interactions)	Energy Score	RMSD Value	H bond (distance Å)
7a		LEU88, GLY89, VAL96,	-8.40	1.02	O of Carbonyl with H of NH of ALA162 (1.993)
7b		LEU88, ALA162, GLU166	-8.79	1.74	None
7c		LEU88, GLY89, GLU166	-8.48	0.28	O of Carbonyl with H of NH of ALA162 (2.120)
7d		LEU88, VAL96, ALA162	-9.37	0.50	O of Carbonylwith H of NH of GLY165 (1.730)
7e		LEU88, VAL96, ALA162	-8.51	1.62	None
8a		LEU88, ALA162, THR222	-8.32	1.54	None
8b		GLY89, VAL96, ALA162, LEU212	-9.13	0.71	H of NH with Carbonyl of LEU88 (1.871)
8c		LEU88, GLY89, LEU212	-8.71	1.18	O of Carbonyl with H of NH of ALA162 (1.915)
8d		LEU88, VAL96, GLU166	-8.61	0.42	O of Carbonyl with H of NH of ALA162 (1.933)
8e		GLY89, VAL96, ALA162	-8.55	0.53	None
9a		LEU88, VAL96, ALA162	-7.97	1.39	None
9b		LEU88, VAL96, LEU212	-8.16	1.00	O of Carbonyl with H of NH of ALA162 (2.113)
9c		LEU88, VAL96, GLU166	-7.96	1.74	O of Carbonyl with H of NH of ALA162 (1.914)
9d		LEU88, VAL96, ALA162	-8.16	1.03	None
9e		LEU88, VAL96, ALA162	-7.28	1.83	None
Doxorubicin		LEU88, ALA162, LEU212	-12.30	0.54	O of Carbonyl with H of NH of GLU166 (2.184)
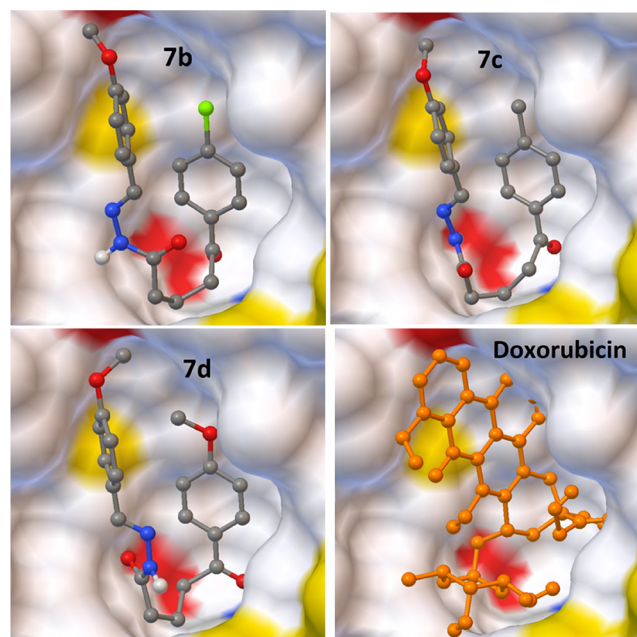
Figure 4. Interaction of the best-docked poses of the reference drug doxorubicin and compounds **7b-d** with the 1X7B target.

Figure 5. Superimposing poses of best-scored compounds with and without reference drug doxorubicin against breast cancer.

selective antiproliferative activity in cancer cells. When the results obtained were evaluated, it was determined that all compounds had cytotoxic activity against cancer cell lines (MCF-7 and PC-3) with IC_{50} values ranging from 7.52 ± 0.32 to 672.18 ± 2.69 μM. Besides, no antiproliferative effect was observed in healthy cells at this dose range. This result shows that all synthesized compounds have selective cytotoxic properties. Compounds **7a-e** were found to have stronger cytotoxic activity in cancer cells than compounds **8a-e** and **9a-e**. Among compounds **7a-e**, it was determined that compound **7d** was the most active compound with IC_{50} values at 7.52 ± 0.32 and 10.19 ± 0.52 μM against MCF-7 and PC-3 cells, respectively. Moreover, **7d** showed no cytotoxic effect on ME-16C cells at the same concentration, although it strongly inhibited the growth of cancer cell lines. Among the selected cancer cell lines, breast cancer (MCF-7) cells were found to be more sensitive to the antiproliferative effects of newly synthesized N-acyl hydrazones.

Molecular docking experiments were used to explore the antiproliferative properties of these new compounds, and appropriate binding free energies of almost all compounds for MCF-7 and PC-3 were determined between −9.67 and −11.74 and −7.28 and −9.37 Kcal/mol, respectively. According to the

Figure 6. Interaction of the best-docked poses of compounds **7b**, **7d**, **8b** and reference drug doxorubicin to 1Z5M target.

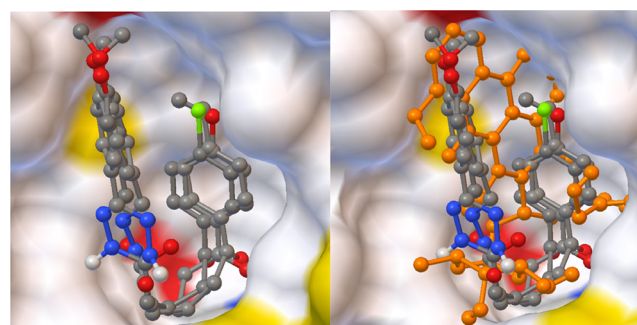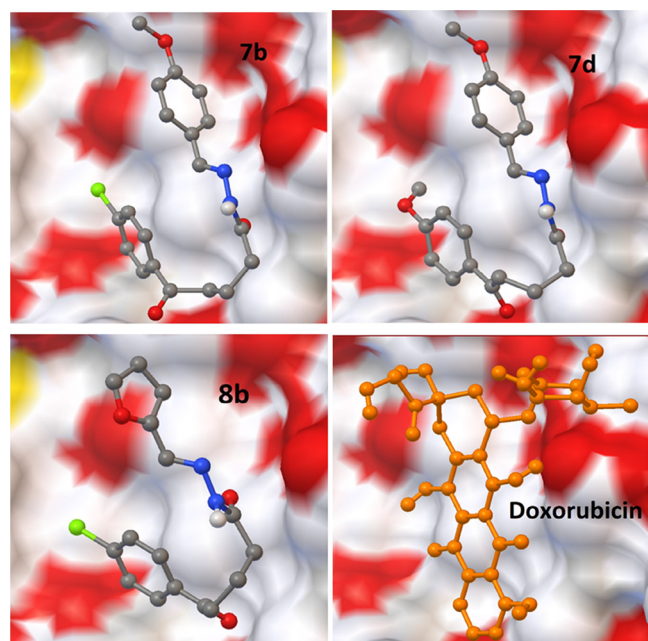**Figure 7.** Superimpsing poses of best-scored compounds with and without reference drug doxorubicin against prostate cancer.
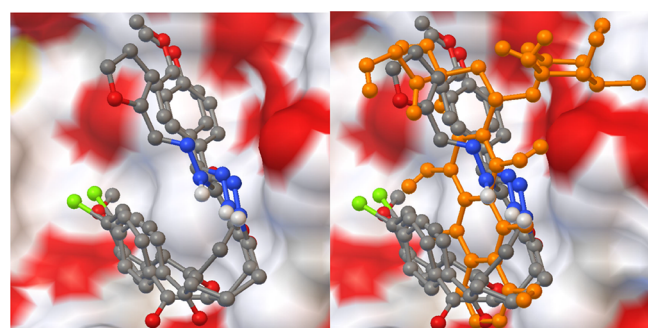
results obtained from molecular docking studies, it was determined that all synthesized *N*-acyl hydrazone derivatives exhibited very good ligand-receptor binding interactions. It has also been discovered that all compounds have relatively favorable values for crossing lipid barriers (lipophilicity value <4).

Since conventional chemotherapy drugs are highly toxic to normal cells, newly synthesized *N*-acyl hydrazone derivatives could be promising candidates for anticancer drug development through their selective cytotoxic activity. Therefore, the potential anticancer efficacy and mechanism of action of *N*-acyl hydrazone derivatives must be further investigated in vivo.

4. EXPERIMENTAL SECTION

4.1. Materials and Apparatuses. All of the chemicals and solvents utilized in the syntheses and in vitro tests were obtained from commercial suppliers (Merck, Sigma-Aldrich, Acros Organics, and Thermo Fisher Scientific) and used without additional purification. Solvents used for chromatography were of technical grade and distilled before use. Thin-layer chromatography (TLC) was used to monitor chemical reactions under 254 nm UV light. The synthesized starting compounds and *N*-acyl hydrazones were purified using column

chromatography on silica gel (0.063–0.200 mm) with hexane-ethylacetate. Melting points were measured with a Buchi melting point apparatus B-540. Gas chromatography–mass spectrometry (GC–MS) data were recorded on a Shimadzu QP2010 Plus. The purity of the *N*-acyl hydrazone derivatives was determined on the Shimadzu/DGU-20A5 HPLC apparatus. FT-IR spectra were recorded on Bruker Vertex. ^{1}H NMR and ^{13}C NMR spectra were recorded at 500 and 126 MHz, respectively. DMSO d_6 was used as a solvent, and Me_4Si was used as the internal standard. LC–MS data were recorded on Shimadzu 8040.

4.2. Synthesis. *4.2.1. General Procedure for the Protection of Methyl δ-Oxo Pentanoate Derivatives (2a-e).* To a solution of δ-oxo methyl ester **1a-e** (1 mmol), ethylene glycol (3 mmol), and triethyl orthoformate (3 mmol) in toluene (5 mL) was added *p*-toluenesulfonic acid monohydrate (0.01 mmol). The reaction mixture was heated to reflux for 24 h until all starting material was consumed in the TLC analysis. Next, the reaction mixture was cooled and quenched with a saturated $NaHCO_3$ solution. The mixture was extracted with petroleum ether (40−60 °C) three times. The combined organic phases were washed with saturated NaCl solution and then dried over anhydrous Na_2SO_4 and concentrated under reduced pressure. The products **2a-e** were obtained as yellow oil in a 90−96% yield.

4.2.2. General Procedure for the Synthesis of δ-Ketal Hydrazides (3a-e). The 80% hydrazine monohydrate (3 mL) was added to a solution of protected δ-oxo methyl ester **2a-e** (5 mmol) in absolute ethanol (15 mL) and was stirred at reflux for 6 h. The reaction mixture was monitored by TLC (eluent: hexanes/EtOAc 1:1) and visualized using UV light. After the reaction is complete, the ethanol was removed under reduced pressure. The mixture was extracted with ethyl acetate three times. The organic phase was washed with distilled water, dried over anhydrous Na_2SO_4, and concentrated under reduced pressure. The ketal hydrazides **3a-e** were obtained in a 95−98% isolated yield.

4.2.3. General Procedure for the Synthesis of δ-Ketal N-Acyl Hydrazones (4a-e, 5a-e, 6a-e).[56,57] The δ-ketal hydrazide **3a-e** (1 mmol) and aldehyde (anisaldehyde, furfural, or isovaleraldehyde) (2 mmol) in DMF (2 mL) were added to a reaction flask, and then the mixture was heated to reflux. The reaction progress was monitored by TLC (eluent: hexane:E-tOAc (1:1). After finishing the reaction, the solvent was removed under reduced pressure. The crude product was purified by column chromatography on silica gel (eluent: hexanes/EtOAc 3:1). The pure products **4a-e**, **5a-e**, and **6a-e** were obtained in 51−95% isolated yields.

4.2.4. General Procedure for the Synthesis of N-Acyl Hydrazone Derivatives by Deprotection of δ-Ketal N-Acyl Hydrazones (7a-e, 8a-e, 9a-e). A solution of δ-ketal *N*-acyl hydrazones **4a-e**, **5a-e**, **6a-e** (1 mmol) and $Bi(NO_3)_3 \cdot 5H_2O$ (0.25 mmol) in CH_2Cl_2 (5 mL) was stirred at room temperature for 2−4 h. Next, the mixture was filtered, and the filtrate was washed first with a 10% aqueous $NaHCO_3$ solution and then with saturated NaCl, dried over anhydrous Na_2SO_4, and concentrated under reduced pressure. The pure products **7a-e**, **8a-e**, and **9a-e** were obtained in a 98% isolated yield.

4.3. HPLC Analysis. The purity of the target compounds was defined by normal phase high-performance liquid chromatography (HPLC) using a 250 × 4,6 mm, 5 μm AD-H chiral column using Hekzan/isopropanol (70:30). The
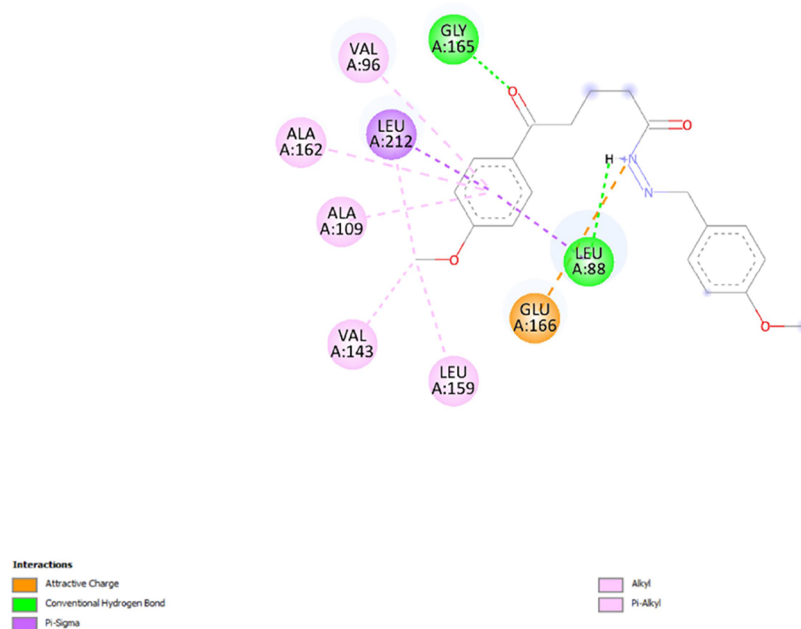
Figure 8. 2D diagram of interactions involved between 1Z5M and **7d**.
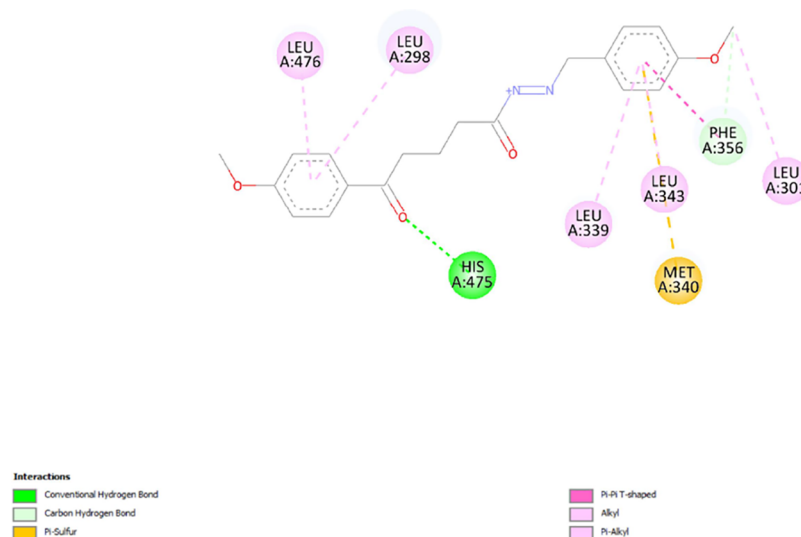
Figure 9. 2D diagram of interactions involved between 1X7B and **7d**.

sample (10 μL) was injected into the column with 1 mL/min flow rate.

4.4. Biological Section. *4.4.1. Cell Culture.* Human breast cancer (MCF-7; ATCC Number: HTB-22), prostate cancer (PC-3; ATCC Number: CRL-1435), and breast epithelial (ME-16C; ATCC Number: CRL: 4101) cell lines were procured from American Type Culture Collection (ATCC Distributor: LGC Standards, Wessel, Germany) to be used in the cytotoxic activity assays. Cells were detached with a 0.25% Trypsin/EDTA solution upon 70−80% confluency and seeded into a new culture flask including DMEM-LG with 10% FBS and 0.1 mg/mL primocin, incubated in a 37 °C, 5% CO_2 incubator. The medium was refreshed every 48 h, and the cells were passaged every 5−6 days.

4.4.2. MTT Assay. Newly synthesized compounds were tested for their cytotoxic activity on cancer (MCF-7, PC-3) and normal (ME-16C) cell lines using the MTT assay. MTT is used to assess cell viability by determining the mitochondrial

activity of living cells according to their ability to reduce the yellow tetrazolium salt MTT into purple formazan crystals. The MTT assay (Thermo) was carried out according to the manufacturer's instructions. Briefly, cells were seeded on 96-well plates at a density of 1×10^4 cells/well and incubated in a 37 °C, 5% CO_2 incubator. Cells were then treated with different concentrations (1−1000 μM) of compounds for 48 h. Following incubation, 10 μL of MTT solution was added to the cells and incubated for 4 h, and then 100 μL of solubilization solution was added and incubated overnight. Absorbance was measured at 570 nm using the microplate reader (Synergy H1, Biotek). For all experiments, doxorubicin was used as the positive control, and untreated cells were used as the negative control. DMSO was used as the solvent of the compounds, and the final concentration did not exceed 0.5% v/v. All the experiments were performed three times, and each was carried out in triplicate.

Table 6. Drug-like Characteristics of Compounds 7a-e, 8a-e, and 9a-e Computed by the Swiss ADME Online Software Program

comp no.	M_W (g/mol)[a]	Log$P$[b]	TPSA[c]	BB[d]	GI Abs[e]	type of CYP Inh[f]	rule of five[g]
7a	324.37	2.98	67.76 Å	yes	high	CYP1A2, CYP2C19, CYP2D6	yes
7b	358.82	3.57	67.76 Å	yes	high	CYP1A2, CYP2C19, CYP2C9, CYP2D6, CYP3A4	yes
7c	338.40	3.30	67.76 Å	yes	high	CYP1A2, CYP2C19, CYP2D6, CYP3A4	yes
7d	354.40	2.98	76.99 Å	yes	high	CYP1A2, CYP2C19, CYP2D6, CYP3A4	yes
7e	330.40	3.04	96.00 Å	no	high	CYP1A2, CYP2C19, CYP2C9	yes
8a	284.31	2.32	71.67 Å	yes	high	CYP1A2, CYP2C19, CYP2C9	yes
8b	318.75	2.84	71.67 Å	yes	high	CYP1A2, CYP2C19, CYP2C9	yes
8c	298.34	2.66	71.67 Å	yes	high	CYP1A2, CYP2C19, CYP2C9	yes
8d	314.34	2.26	80.90 Å	no	high	CYP1A2, CYP2C19, CYP2C9	yes
8e	290.34	2.38	99.91 Å	no	high	CYP1A2, CYP2C19, CYP2C9	yes
9a	274.36	2.90	58.53 Å	yes	high	CYP2C19	yes
9b	308.80	3.39	58.53 Å	yes	high	CYP1A2, CYP2C19	yes
9c	288.38	3.21	58.53 Å	yes	high	CYP2C19	yes
9d	304.38	2.90	67.76 Å	yes	high	CYP1A2	yes
9e	280.39	2.78	86.77 Å	no	high	CYP1A2, CYP2C19	yes
doxorubicin	543.52	1.31	206.07 Å	no	low	none	no

[a]Molecular weight (recommended value <500). [b]Logarithm of the partition coefficient of the compound between n-octanol and water (recommended value <5). [c]Polar surface area (recommended value ≤140 Å²). [d]Indicates whether the compound passes BBB or not. [e]Degree of gastrointestinal absorption. [f]Represents the inhibition of CYP450 subtypes. [g]Indicates whether the compound obeys Lipinski's rule of five or not.

4.5. Molecular Docking Procedure. To provide a theoretical perspective on probable molecular interactions between compounds from the 7a-e, 8a-e, and 9a-e series and target proteins, molecular docking experiments were conducted. Energy minimization was used to calculate theoretical binding affinities based on the results of docking calculations. The computation of molecular docking, energy reduction, and molecular visualization of docking data was carried out using the Autodock Vina software suite. The Chem Draw drawing program was used to prepare model inhibitor compounds for molecular docking in the 7a-e, 8a-e, and 9a-e series. Before the docking procedure, the special 7a-e, 8a-e, and 9a-e series compounds were drawn and edited in the SD File format using the Chem 3D suite program. Protonation, charging, and conformation minimization utilizing the root-mean-square gradient have all been applied to these molecular structures.

Three-dimensional coordinates of X-ray crystal structures of target proteins were obtained from the Structural Bioinformatics Research Collaboration (RCSB) Protein Data Bank.[62] For use in docking calculations, a structure with the PDB IDs 1X7B for MCF-7 and 1Z5M for PC-3 was selected as the crystal structure model matching these target proteins. The software tool Autodock Vina was used to correct structural defects in these target proteins. As docking calculations are being performed, default parameters are being used (temperature 300 Kelvin, pH 7, solvent 0.1 M, electrostatic energy cutoff 15 A). The final molecular docking score values were calculated using the average score of the top 10 final docking postures determined by the binding minimum energy (kcal/mol) for each molecule.[62,63]

ASSOCIATED CONTENT

Supporting Information

The Supporting Information is available free of charge at https://pubs.acs.org/doi/10.1021/acsomega.3c02361.

> Experimental details; general procedures; experimental characterization data (IR, NMR, LC−MS, and HPLC purity); HPLC chromatograms; FT-IR spectra and ^{1}H, ^{13}C NMR spectra of all target products (PDF)

AUTHOR INFORMATION

Corresponding Author

Belma Hasdemir − *Department of Chemistry, Organic Chemistry Division, Istanbul University-Cerrahpaşa, Istanbul 34320, Turkey;* ⊙ orcid.org/0000-0002-1071-1127; Email: b.hasdemir@iuc.edu.tr

Authors

Yağmur Biliz − *Institute of Graduate Studies, Istanbul University-Cerrahpaşa, Istanbul 34320, Turkey*

Hatice Başpınar Küçük − *Department of Chemistry, Organic Chemistry Division, Istanbul University-Cerrahpaşa, Istanbul 34320, Turkey*

Merve Zaim − *SANKARA Brain and Biotechnology Research Center, Entertech Technocity, Istanbul 34320, Turkey*

Ahmet Mesut Şentürk − *Department of Pharmeceutical Chemistry, Faculty of Pharmacy, Istanbul Biruni University, Istanbul 34010, Turkey*

Aynur Müdüroğlu Kırmızıbekmez − *Department of Physical Therapy and Rehabilitation, School of Health Sciences, Nisantasi University, Istanbul 34398, Turkey*

İhsan Kara − *SANKARA Brain and Biotechnology Research Center, Entertech Technocity, Istanbul 34320, Turkey*

Complete contact information is available at:
https://pubs.acs.org/10.1021/acsomega.3c02361

Notes

The authors declare no competing financial interest.

ACKNOWLEDGMENTS

REFERENCES

(1) Ghouri, Y.; Mian, I.; Rowe, J. Review of Hepatocellular Carcinoma: Epidemiology, Etiology, and Carcinogenesis. *J. Carcinog.* **2017**, *16*, 1.

(2) Popiołek, Ł.; Gawrońska-Grzywacz, M.; Berecka-Rycerz, A.; Paruch, K.; Piątkowska-Chmiel, I.; Natorska-Chomicka, D.; Herbet, M.; Gumieniczek, A.; Dudka, J.; Wujec, M. New Benzenesulphonohy-drazide Derivatives as Potential Antitumour Agents. *Oncol. Lett.* **2020**, *20*, 136.

(3) Sung, H.; Ferlay, J.; Siegel, R. L.; Laversanne, M.; Soerjomataram, I.; Jemal, A.; Bray, F. Global Cancer Statistics 2020: GLOBOCAN Estimates of Incidence and Mortality Worldwide for 36 Cancers in 185 Countries. *CA, Cancer J. Clin.* **2021**, *71*, 209−249.

(4) Duma, N.; Santana-Davila, R.; Molina, J. R. Non−Small Cell Lung Cancer: Epidemiology, Screening, Diagnosis, and Treatment. *Mayo Clin. Proc.* **2019**, *94*, 1623−1640.

(5) Singh, V.; Srivastava, V. K.; Palit, G.; Shanker, K. Coumarin Congeners as Antidepressants. *Arzneimittelforschung* **1992**, *42*, 993−996.

(6) Rollas, S.; Küçükgüzel, S. Biological Activities of Hydrazone Derivatives. *Molecules* **2007**, *12*, 1910−1939.

(7) Küçükgüzel, S. G.; Mazi, A.; Sahin, F.; Öztürk, S.; Stables, J. Synthesis and Biological Activities of Diflunisal Hydrazide−Hydrazones. *Eur. J. Med. Chem.* **2003**, *38*, 1005−1013.

(8) Seleem, H. S.; El-Inany, G. A.; El-Shetary, B. A.; Mousa, M. A.; Hanafy, F. I. The Ligational Behavior of a Phenolic Quinolyl Hydrazone towards Copper(II)-Ions. *Chem. Cent. J.* **2011**, *5*, 2−9.

(9) Bushra; Shamim, S.; Khan, K. M.; Ullah, N.; Mahdavi, M.; Faramarzi, M. A.; Larijani, B.; Salar, U.; Rafique, R.; Taha, M.; Perveen, S. Synthesis, in Vitro, and in Silico Evaluation of Indazole Schiff Bases as Potential α-Glucosidase Inhibitors. *J. Mol. Struct.* **2021**, *1242*, No. 130826.

(10) Salar, U.; Qureshi, B.; Khan, K. M.; Lodhi, M. A.; Ul-Haq, Z.; Khan, F. A.; Naz, F.; Taha, M.; Perveen, S.; Hussain, S. Aryl Hydrazones Linked Thiazolyl Coumarin Hybrids as Potential Urease Inhibitors. *J. Iran. Chem. Soc.* **2022**, *19*, 1221−1238.

(11) Khan, I.; Rehman, W.; Rahim, F.; Hussain, R.; Khan, S.; Fazil, S.; Rasheed, L.; Taha, M.; Shah, S. A. A.; Abdellattif, M. H.; Farghaly, T. A. Synthesis, In Vitro α-Glucosidase Inhibitory Activity and Molecular Docking Study of New Benzotriazole-Based Bis-Schiff Base Derivatives. *Pharmaceuticals* **2023**, *16*, 17.

(12) Ullah, H.; Uddin, I.; Rahim, F.; Khan, F.; Sobia; Taha, M.; Khan, M. U.; Hayat, S.; Ullah, M.; Gul, Z.; Ullah, S.; Zada, H.; Hussain, J. In Vitro α-Glucosidase and α-Amylase Inhibitory Potential and Molecular Docking Studies of Benzohydrazide Based Imines and Thiazolidine-4-One Derivatives. *J. Mol. Struct.* **2022**, *1251*, No. 132058.

(13) Ali, I.; Rafique, R.; Khan, K. M.; Chigurupati, S.; Ji, X.; Wadood, A.; Rehman, A. U.; Salar, U.; Alyamani, N. M.; Hameed, S.; Taha, M.; Hussain, S.; Perveen, S. Benzofuran Hybrids as Cholinesterase (AChE and BChE) Inhibitors: In Vitro, In Silico, and Kinetic Studies. *Russ. J. Bioorg. Chem.* **2022**, *48*, 1322−1337.

(14) Nikolova-Mladenova, B.; Momekov, G.; Ivanov, D.; Bakalova, A. Design and Drug-like Properties of New 5-Methoxysalicylaldehyde Based Hydrazones with Anti-Breast Cancer Activity. *J. Appl. Biomed.* **2017**, *15*, 233−240.

(15) Tantak, M. P.; Klingler, L.; Arun, V.; Kumar, A.; Sadana, R.; Kumar, D. Design and Synthesis of Bis(Indolyl)Ketohydrazide-Hydrazones: Identification of Potent and Selective Novel Tubulin Inhibitors. *Eur. J. Med. Chem.* **2017**, *136*, 184−194.

(16) Patil, S.; Mahesh Kuman, M.; Palvai, S.; Sengupta, P.; Basu, S. Impairing Powerhouse in Colon Cancer Cells by Hydrazide−Hydrazone-Based Small Molecule. *ACS Omega* **2018**, *3*, 1470−1481.

(17) Nasr, T.; Bondock, S.; Rashed, H. M.; Fayad, W.; Youns, M.; Sakr, T. M. Novel Hydrazide-Hydrazone and Amide Substituted Coumarin Derivatives: Synthesis, Cytotoxicity Screening, Microarray, Radiolabeling and in Vivo Pharmacokinetic Studies. *Eur. J. Med. Chem.* **2018**, *151*, 723−739.

(18) Sreenivasulu, R.; Reddy, K. T.; Sujitha, P.; Kumar, C. G.; Raju, R. R. Synthesis, Antiproliferative and Apoptosis Induction Potential Activities of Novel Bis(Indolyl)Hydrazide-Hydrazone Derivatives. *Bioorg. Med. Chem.* **2019**, *27*, 1043−1055.

(19) Mohareb, R. M.; El-Sharkawy, K. A.; Al Farouk, F. O. Synthesis, Cytotoxicity against Cancer and Normal Cell Lines of Novel Hydrazide-Hydrazone Derivatives Bearing 5H-Chromen-5-One. *Med. Chem. Res.* **2019**, *28*, 1885−1900.

(20) Han, M. İ.; Bekçi, H.; Uba, A. I.; Yıldırım, Y.; Karasulu, E.; Cumaoğlu, A.; Karasulu, H. Y.; Yelekçi, K.; Yılmaz, Ö.; Küçükgüzel, Ş. G. Synthesis, Molecular Modeling, in Vivo Study, and Anticancer Activity of 1,2,4-triazole Containing Hydrazide−Hydrazones Derived from (S)-naproxen. *Arch. Pharm.* **2019**, *352*, No. 1800365.

(21) Noma, S. A. A.; Erzengin, M.; Tunç, T.; Balcıoğlu, S. Synthesis, Characterization and Biological Assessment of a Novel Hydrazone as Potential Anticancer Agent and Enzyme Inhibitor. *J. Mol. Struct.* **2020**, *1205*, No. 127550.

(22) Patil, S.; Pandey, S.; Singh, A.; Radhakrishna, M.; Basu, S. Hydrazide−Hydrazone Small Molecules as AIEgens: Illuminating Mitochondria in Cancer Cells. *Chem. − Eur. J.* **2019**, *25*, 8229−8235.

(23) Alotabi, S. H. Synthesis, Characterization, Anticancer Activity, and Molecular Docking of Some New Sugar Hydrazone and Arylidene Derivatives. *Arab. J. Chem.* **2020**, *13*, 4771−4784.

(24) Popiołek, Ł.; Piątkowska-Chmiel, I.; Gawrońska-Grzywacz, M.; Biernasiuk, A.; Izdebska, M.; Herbet, M.; Sysa, M.; Malm, A.; Dudka, J.; Wujec, M. New Hydrazide-Hydrazones and 1,3-Thiazolidin-4-Ones with 3-Hydroxy-2-Naphthoic Moiety: Synthesis, in Vitro and in Vivo Studies. *Biomed. Pharmacother.* **2018**, *103*, 1337−1347.

(25) İhsan Han, M.; Atalay, P.; İmamoğlu, N.; Küçükgüzel, Ş. G. Synthesis, Characterization and Anticancer Activity of Novel Hydrazide-Hydrazones Derived from Ethyl Paraben. *J. Res. Pharm.* **2020**, *24*, 341−349.

(26) Gautam, A.; Rawat, P.; Singh, R. N.; Flores Holguin, N. R. Synthesis, Spectroscopic and Evaluation of Anticancer Activity of New Hydrazone-Containing Dipyrromethane Using Experimental and Theoretical Approaches. *J. Mol. Struct.* **2022**, *1260*, No. 132781.

(27) Koç, H. C.; Atlihan, İ.; Mega-Tiber, P.; Orun, O.; Güniz Küçükgüzel, Ş. Synthesis of Some Novel Hydrazide-Hydrazones Derived from Etodolac as Potential Anti-Prostate Cancer Agents. *J. Res. Pharm.* **2022**, *26*, 1−12.

(28) Angelova, V. T.; Vassilev, N. G.; Nikolova-Mladenova, B.; Vitas, J.; Malbaša, R.; Momekov, G.; Djukic, M.; Saso, L. Antiproliferative and Antioxidative Effects of Novel Hydrazone Derivatives Bearing Coumarin and Chromene Moiety. *Med. Chem. Res.* **2016**, *25*, 2082−2092.

(29) Anastassova, N. O.; Yancheva, D. Y.; Mavrova, A. T.; Kondeva-Burdina, M. S.; Tzankova, V. I.; Hristova-Avakumova, N. G.; Hadjimitova, V. A. Design, Synthesis, Antioxidant Properties and Mechanism of Action of New N,N′-Disubstituted Benzimidazole-2-Thione Hydrazone Derivatives. *J. Mol. Struct.* **2018**, *1165*, 162−176.

(30) Sıcak, Y.; Oruç-Emre, E. E.; Öztürk, M.; Taşkın-Tok, T.; Karaküçük-Iyidoğan, A. Novel Fluorine-Containing Chiral Hydrazide-Hydrazones: Design, Synthesis, Structural Elucidation, Antioxidant and Anticholinesterase Activity, and in Silico Studies. *Chirality* **2019**, *31*, 603−615.

(31) Pham-Huy, L. A.; He, H.; Pham-Huy, C. Free Radicals, Antioxidants in Disease and Health. *Int. J. Biomed. Sci.* **2008**, *4*, 89−96.

(32) Navidpour, L.; Shafaroodi, H.; Saeedi-Motahar, G.; Shafiee, A. Synthesis, Anti-Inflammatory and Analgesic Activities of Arylidene-2-(3-Chloroanilino)Nicotinic Acid Hydrazides. *Med. Chem. Res.* **2014**, *23*, 2793−2802.

(33) Moldovan, C. M.; Oniga, O.; Pârvu, A.; Tiperciuc, B.; Verite, P.; Pîrnǎu, A.; Crişan, O.; Bojiţǎ, M.; Pop, R. Synthesis and Anti-Inflammatory Evaluation of Some New Acyl-Hydrazones Bearing 2-Aryl-Thiazole. *Eur. J. Med. Chem.* **2011**, *46*, 526−534.

(34) Kumar Reddy, A. L. V.; Kathale, N. E. Synthesis and Anti-Inflammatory Activity of Hydrazide-Hydrazones Bearing Anacardic Acid and 1,2,3-Triazole Ring Based Hybrids. *Orient. J. Chem.* **2017**, *33*, 2930−2936.

(35) Meira, C. S.; dos Santos Filho, J. M.; Sousa, C. C.; Anjos, P. S.; Cerqueira, J. V.; Dias Neto, H. A.; da Silveira, R. G.; Russo, H. M.; Wolfender, J. L.; Queiroz, E. F.; Moreira, D. R. M.; Soares, M. B. P.

Structural Design, Synthesis and Substituent Effect of Hydrazone-N-Acylhydrazones Reveal Potent Immunomodulatory Agents. *Bioorg. Med. Chem.* **2018**, *26*, 1971−1985.

(36) Popiołek, Ł. Hydrazide-Hydrazones as Potential Antimicrobial Agents: Overview of the Literature since 2010. *Med. Chem. Res.* **2017**, *26*, 287−301.

(37) Krátký, M.; Bősze, S.; Baranyai, Z.; Stolaříková, J.; Vinšová, J. Synthesis and Biological Evolution of Hydrazones Derived from 4-(Trifluoromethyl)Benzohydrazide. *Bioorg. Med. Chem. Lett.* **2017**, *27*, 5185−5189.

(38) Pham, V. H.; Phan, T. P. D.; Phan, D. C.; Vu, B. D. Synthesis and Bioactivity of Hydrazide-Hydrazones with the 1-Adamantyl-Carbonyl Moiety. *Molecules* **2019**, *24*, 4000.

(39) Haiba, N. S.; Khalil, H. H.; Moniem, M. A.; El-Wakil, M. H.; Bekhit, A. A.; Khattab, S. N. Design, Synthesis and Molecular Modeling Studies of New Series of s-Triazine Derivatives as Antimicrobial Agents against Multi-Drug Resistant Clinical Isolates. *Bioorg. Chem.* **2019**, *89*, No. 103013.

(40) Ajani, O. O.; Iyaye, K. T.; Aderohunmu, D. V.; Olanrewaju, I. O.; Germann, M. W.; Olorunshola, S. J.; Bello, B. L. Microwave-Assisted Synthesis and Antibacterial Propensity of N′-s-Benzylidene-2-Propylquinoline-4-Carbohydrazide and N′-((s-1H-Pyrrol-2-Yl)-Methylene)-2-Propylquinoline-4-Carbohydrazide Motifs. *Ar. J. Chem.* **2020**, *13*, 1809−1820.

(41) Rohane, S. H.; Chauhan, A. J.; Fuloria, N. K.; Fuloria, S. Synthesis and in Vitro Antimycobacterial Potential of Novel Hydrazones of Eugenol. *Ar. J. Chem.* **2020**, *13*, 4495−4504.

(42) Senkardes, S.; Kaushik-Basu, N.; Durmaz, I.; Manvar, D.; Basu, A.; Atalay, R.; Guniz Kucukguzel, S. Synthesis of Novel Diflunisal Hydrazide−Hydrazones as Anti-Hepatitis C Virus Agents and Hepatocellular Carcinoma Inhibitors. *Eur. J. Med. Chem.* **2016**, *108*, 301−308.

(43) Gürsoy, E.; Dincel, E. D.; Naesens, L.; Ulusoy Güzeldemirci, N. Design and Synthesis of Novel Imidazo[2,1-b]Thiazole Derivatives as Potent Antiviral and Antimycobacterial Agents. *Bioorg. Chem.* **2020**, *95*, No. 103496.

(44) Dehestani, L.; Ahangar, N.; Hashemi, S. M.; Irannejad, H.; Honarchian Masihi, P.; Shakiba, A.; Emami, S. Design, Synthesis, in Vivo and in Silico Evaluation of Phenacyl Triazole Hydrazones as New Anticonvulsant Agents. *Bioorg. Chem.* **2018**, *78*, 119−129.

(45) Inam, A.; Siddiqui, S. M.; Macedo, T. S.; Moreira, D. R. M.; Leite, A. C. L.; Soares, M. B. P.; Azam, A. Design, Synthesis and Biological Evaluation of 3-[4-(7-Chloro-Quinolin-4-Yl)-Piperazin-1-Yl]-Propionic Acid Hydrazones as Antiprotozoal Agents. *Eur. J. Med. Chem.* **2014**, *75*, 67−76.

(46) Bekhit, A. A.; Saudi, M. N.; Hassan, A. M. M.; Fahmy, S. M.; Ibrahim, T. M.; Ghareeb, D.; El-Seidy, A. M.; Nasralla, S. N.; Bekhit, A. E.-D. A. Synthesis, in Silico Experiments and Biological Evaluation of 1,3,4-Trisubstituted Pyrazole Derivatives as Antimalarial Agents. *Eur. J. Med. Chem.* **2019**, *163*, 353−366.

(47) Akdag, K.; Kocyigit-Kaymakcioglu, B.; Tabanca, N.; Ali, A.; Estep, A.; Becnel, J. J.; Khan, I. A. Synthesis and Larvicidal and Adult Topical Activity of Some Hydrazide-Hydrazone Derivatives against Aedes Aegypti. *Marmara Pharm. J.* **2014**, *3*, 120−125.

(48) Pavan, F. R.; da S. Maia, P. I.; Leite, S. R. A.; Deflon, V. M.; Batista, A. A.; Sato, D. N.; Franzblau, S. G.; Leite, C. Q. F. Thiosemicarbazones, Semicarbazones, Dithiocarbazates and Hydrazide/Hydrazones: Anti − Mycobacterium Tuberculosis Activity and Cytotoxicity. *Eur. J. Med. Chem.* **2010**, *45*, 1898−1905.

(49) Backes, G. L.; Neumann, D. M.; Jursic, B. S. Synthesis and Antifungal Activity of Substituted Salicylaldehyde Hydrazones, Hydrazides and Sulfohydrazides. *Bioorg. Med. Chem.* **2014**, *22*, 4629−4636.

(50) Hasdemir, B.; Yaşa, H.; Akkamış, Y. Synthesis and Antioxidant Activities of Novel N-Aryl (and N-Alkyl) γ-and δ-Imino Esters and Ketimines. *J. Chin. Chem. Soc.* **2018**, *66*, 197−204.

(51) Hasdemir, B.; Sacan, O.; Yasa, H.; Kucuk, H. B.; Yusufoglu, A. S.; Yanardag, R. Synthesis and Elastase Inhibition Activities of Novel Aryl, Substituted Aryl, and Heteroaryl Oxime Ester Derivatives. *Arch. Pharm.* **2018**, *351*, No. e1700269.

(52) Maekawa, T.; Sakai, N.; Tawada, H.; Murase, K.; Hazama, M.; Sugiyama, Y.; Momose, Y. Synthesis and Biological Activity of Novel 5-(.OMEGA.-Aryloxyalkyl)Oxazole Derivatives as Brain-Derived Neurotrophic Factor Inducers. *Chem. Pharm. Bull.* **2003**, *51*, 565−573.

(53) Raposo, M. M. M.; Kirsch, G. A Combination of Friedel-Crafts and Lawesson Reactions to 5-Substituted-2, 2′-Bithiophenes. *Heterocycles* **2001**, *55*, 1487−1498.

(54) Aydoğan, F.; Turgut, Z.; Öcal, N.; Erdem, Safiye Sağ Synthesis and Electronic Structure of New Aryl-and Alkyl-Substituted 1,3,4-Oxadiazole-2-Thione Derivatives. *Turk. J. Chem.* **2002**, *26*, 1−11.

(55) Abu-Hashem, A. A. Synthesis of New Pyrazoles, Oxadiazoles, Triazoles, Pyrrolotriazines, and Pyrrolotriazepines as Potential Cytotoxic Agents. *J. Heterocycl. Chem.* **2021**, *58*, 805−821.

(56) Aydın, E.; Şentürk, A. M.; Küçük, H. B.; Güzel, M. Cytotoxic Activity and Docking Studies of 2-Arenoxybenzaldehyde N-Acyl Hydrazone and 1,3,4-Oxadiazole Derivatives against Various Cancer Cell Lines. *Molecules* **2022**, *27*, 7309.

(57) Küçük, H. B.; Alhonaish, A.; Yıldız, T.; Güzel, M. An Efficient Approach to Access 2,5-Disubstituted 1,3,4-Oxadiazoles by Oxidation of 2-Arenoxybenzaldehyde N-Acyl Hydrazones with Molecular Iodine. *ChemistrySelect* **2022**, *7*, No. e202201391.

(58) Giancotti, G.; Cancellieri, M.; Balboni, A.; Giustiniano, M.; Novellino, E.; Delang, L.; Neyts, J.; Leyssen, P.; Brancale, A.; Bassetto, M. Rational Modifications on a Benzylidene-Acrylohydrazide Antiviral Scaffold, Synthesis and Evaluation of Bioactivity against Chikungunya Virus. *Eur. J. Med. Chem.* **2018**, *149*, 56−68.

(59) Bartmańska, A.; Tronina, T.; Popłoński, J.; Milczarek, M.; Filip-Psurska, B.; Wietrzyk, J. Highly Cancer Selective Antiproliferative Activity of Natural Prenylated Flavonoids. *Molecules* **2018**, *23*, 2922.

(60) Poutiainen, P. K.; Venäläinen, T. A.; Peräkylä, M.; Matilainen, J. M.; Väisänen, S.; Honkakoski, P.; Laatikainen, R.; Pulkkinen, J. T. Synthesis and Biological Evaluation of Phenolic 4,5-Dihydroisoxazoles and 3-Hydroxy Ketones as Estrogen Receptor α and β Agonists. *Bioorg. Med. Chem.* **2010**, *18*, 3437−3447.

(61) Lee, A. C.-H.; Ramanujulu, P. M.; Poulsen, A.; Williams, M.; Blanchard, S.; Ma, D. M.; Bonday, Z.; Goh, K. L.; Goh, K. C.; Goh, M. K.; Wood, J.; Dymock, B. W. Thieno[3,2-d]Pyrimidin-4(3H)-One Derivatives as PDK1 Inhibitors Discovered by Fragment-Based Screening. *Bioorg. Med. Chem. Lett.* **2012**, *22*, 4023−4027.

(62) PCSB Protein data bank, RCSB PDB is funded by the National Science Foundation (DBI-1832184).

(63) Swiss Institute of Bioinformatics, **2022**.